Designing Analogues of Mini Atrial Natriuretic Peptide Based on Structural Analysis by NMR and Restrained Molecular Dynamics

Kenji Sugase,[†,‡] Yoshiaki Oyama,[§] Katsuhiko Kitano,[§] Takashi Iwashita,[†] Toshimichi Fujiwara,[‡,||] Hideo Akutsu,*[,‡,||] and Masaji Ishiguro*[,†]

Suntory Institute for Bioorganic Research and Suntory Institute for Biomedical Research, Shimamoto, Mishima 618-8503, Japan, Department of Chemistry and Biotechnology, Faculty of Engineering, Yokohama National University, Hodogaya-ku, Yokohama 240-8501, Japan, and Institute for Protein Research, Osaka University, Yamadaoka, Suita 565-0871, Japan

Received March 8, 2001

Analogues of mini atrial natriuretic peptide (miniANP) that provide conformational properties related to biological activity were designed on the basis of the structure revealed by NMR and restrained molecular dynamics (rMD) simulation, and an analogue with a high level of biological activity was successfully obtained. MiniANP is a cyclic pentadecapeptide analogue of atrial natriuretic polypeptide (ANP). The conformation of miniANP analyzed by NMR and rMD simulation indicated that positive ϕ angles are preferred for Gly^5 and Gly^6, which is typical for D-amino acids. On the basis of the structural information, [D-Ala^5]miniANP, [D-Ala^6]miniANP, and [D-Ala^5 D-Ala^6]miniANP were synthesized. The biological activity of [D-Ala^5]miniANP was stronger than that of miniANP, confirming that Gly^5 of miniANP takes a positive ϕ angle on binding to the receptor. Conformational analysis of these analogue peptides by NMR suggested that a turnlike conformation at residues 6−9 and a proximate pair formed by side chains of Phe^4 and Ile^{11} are important for the biological activity.

Introduction

Mini atrial natriuretic peptide (miniANP (**1**)) is a synthetic peptide analogue of atrial natriuretic polypeptide (ANP (**2**)),[1] which is a potent hypotensive hormone composed of 28 amino acids, regulating fluid balance, electrolyte balance, blood pressure, and the renin−angiotensin system (Figure 1).[2,3] For the purpose of generating a lead compound for drug design, miniANP (**1**) was produced by trimming and optimizing ANP (**2**). The size of the polypeptide was reduced by approximately half, while a high-affinity (one-seventh that of ANP (**2**)) was retained. Met^1, His^3, Phe^4, Gly^5, Gly^6, Arg^7, Met^8, Ile^{11}, Ser^{12}, Tyr^{14}, and Arg^{15} were chosen as the optimum residues by alanine-scanning mutagenesis and monovalent phage display. Alanine-scanning mutagenesis studies applied to the prototype of miniANP (**1**), having the additional sequence Ser^1-Leu^2-Asp^3-Arg^4 at the N terminus, indicated that the most important determinants were Phe^8, Met^{12}, and Ile^{15}, corresponding to Phe^4, Met^8, and Ile^{11} of miniANP (**1**). In particular, replacement of Phe^8 or Ile^{15} by Ala suppressed the binding affinity by more than 1000-fold.[1] MiniANP (**1**) selectively binds to a natriuretic peptide receptor (NPR-A), which is a transmembrane protein composed of approximately 1060 residues. NPR-A contains an extracellular ligand-binding domain, a single transmembrane region, an intracellular kinase-homologous domain, and a guanylate cyclase domain.[4,5] Biochemical studies showed that NPR-A exists as a tetramer form in a ligand-independent fashion.[6−8] Binding of miniANP (**1**) to the extracellular domain of NPR-A activates synthesis of cGMP (cyclic guanosine 5′-monophosphate).[4,5] Most of the physiological activity may be attributed to this activation.

Figure 1. Sequence alignment of ANP, miniANP, and analogue peptides of miniANP. A lower-case letter means a D-amino acid. The residues essential for the biological activity determined by alanine scan mutagenesis are underlined, and the residues chosen by monovalent phage display are in bold.

Since miniANP (**1**) is the smallest of the ANP-related peptides, elucidation of its structure−activity relationship will be useful for characterizing the mechanism for receptor activation and designing smaller non-peptide ligands. Amino acid substitution and deletion have been widely applied to ANP (**2**) for such purposes. For instance, Bovy et al. synthesized nine analogue peptides of ANP to identify the structural requirement for ANP receptor subtypes.[9] These techniques revealed functional groups essential for biological activity but did not explain their roles in binding to a receptor. To design analogues efficiently as well as to understand the biological mechanism, the three-dimensional structure is indispensable. The best way to determine the structure of a ligand−receptor complex is by X-ray crystallography or NMR. However, because of difficulties in obtaining receptors and their preparation for structural

* To whom correspondence should be addressed. Phone: +81-75-962-3742. Fax: +81-75-962-2115. E-mail: ishiguro@sunbor.or.jp.
† Suntory Institute for Bioorganic Research.
‡ Yokohama National University.
§ Suntory Institute for Biomedical Research.
|| Institute for Protein Research.

10.1021/jm010106k CCC: $22.00
Published on Web 01/22/2002

analysis, few receptor proteins are amenable to these methods. Thus, conformational properties related to biological activity are usually inferred from the structural information of a ligand itself. The solution conformation of a ligand would provide a clue as to conformational properties related to biological activity. Although NMR is a suitable method for such investigations, most small peptides would interconvert several conformations rapidly in aqueous solution. NMR encounters difficulty because of time- and ensemble-averaged structural parameters such as the nuclear Overhauser effect (NOE) and the *J* coupling constant. Consequently, NMR studies on biologically active peptides require complementary information.

In this study, conformational properties related to the biological activity of miniANP (**1**) have been investigated by NMR combined with restrained molecular dynamics (rMD) simulation, which led us to design analogue peptides with high activity. We focused on the conformation of Gly^5−Gly^6, which is conserved in the wild-type ANP (**2**) and was chosen as an indispensable region by monovalent phage display.[1]

Results

Solution Conformation of miniANP. NMR analysis of miniANP (**1**) was performed for aqueous and DMSO solutions, since the environment of the binding site of the relevant receptor was not known. The signals of mini ANP (**1**) in the DMSO solution were broader than those in the aqueous solution. Since aggregation of the sample may be the origin of the line broadening, the concentration dependence of miniANP (**1**) was examined in both aqueous and DMSO solutions. The 1D NMR spectra of samples of 0.1, 2.0, and 10.0 mM were measured. No difference between chemical shifts at the three concentrations was detected except for small differences in some exchangeable protons in the DMSO solution due to a difference in the relative amounts of residual water in the solution. Thus, it is concluded that miniANP (**1**) was not aggregated in both solutions. The temperature change showed that the line width becomes narrower with an increase of temperature. The influence of the residual water on the line width was also examined by using a sample in which water was carefully removed, and no appreciable change of the line width was observed. These indicate that the broadening is not due to the proton exchange between the amide and water. Consequently, the broadening might be attributed to the fast exchange among several conformations in the solutions. The exchange rate is not fast enough to give sharp signals. With this in mind, the following NMR analyses were carried out; namely, the obtained structure is not a real structure but an average structure. Therefore, we can only use this structure to extract conformational characteristics, which need to be confirmed by other methods to claim their validity.

Figure 2 shows the fingerprint regions of 2D NOE spectra of miniANP (**1**) in aqueous (A) and DMSO (B) solutions. Intraresidue NH−H^α NOE cross-peaks of Cys^2 and His^3 were not observed in the aqueous solution because of exchange broadening (Figure 2A).

NOE distance restraints are summarized in Table 1, and the medium- and long-range NOE connectivities of miniANP (**1**) in the DMSO solution are given in Table 2. A characteristic NOE connectivity between Gly^6 and Asp^9 was observed in both solutions, while long-range NOE connectivities between Phe^4 and Ile^{11} existed only in the DMSO solution.

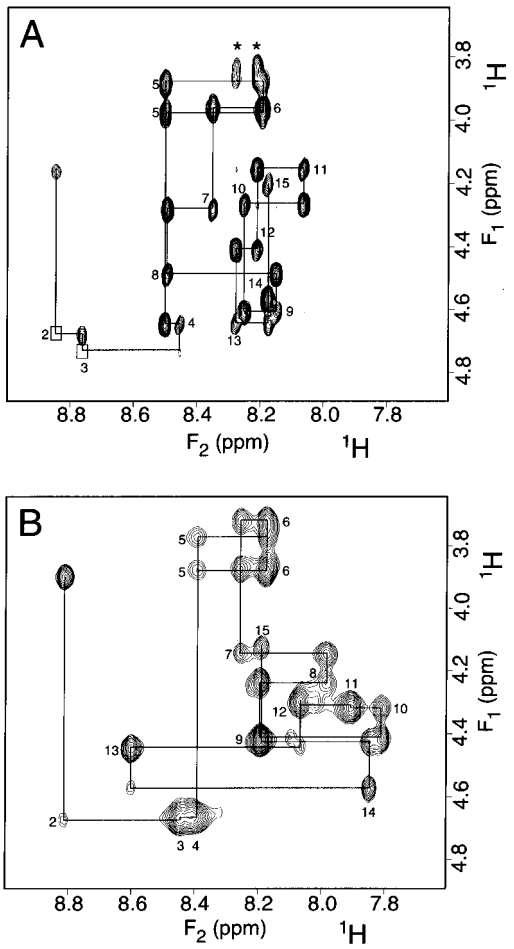

Figure 2. Amide-H^α regions of NOESY spectra of miniANP (**1**) in aqueous (A) and DMSO (B) solutions. The mixing time was 300 ms. The intraresidue $d_{\alpha N}$ NOE cross-peaks are labeled with the residue number, and cross-peaks that disappeared because of exchange broadening are boxed. The $d_{\alpha N}(i,i)$ and $d_{\alpha N}(i,i+1)$ cross-peaks are connected sequentially by the solid lines. The cross-peak indicated by asterisks can be ascribed to Ser^{12} H^β in the F_1 dimension.

Table 1. Distribution of the Observed NOE Connectivities of the Analogue Peptides

peptide	intraresidue	sequential	medium-range[a]	long-range[b]	total
aqueous solution					
1	44	58	9	0	111
3	52	57	13	1	123
4	57	52	5	2	116
5	75	40	8	8	131
DMSO solution					
1	45	63	9	15	132
3	60	74	12	21	167

[a] Medium-range represents links whose sequence separation is between $i + 1$ and $i + 4$. [b] Long-range represents restraint links whose sequence separation is greater than four residues.

A simulated annealing calculation was started with 50 initial conformations, and the 10 lowest energy conformations were used in the subsequent analysis. Pairwise root-mean-square deviations (rmsd) of the

Table 2. Medium- and Long-Range NOE Connectivities of MiniANP (**1**) in DMSO Solution

medium-range NOE connectivity				
proton		−proton		NOE restraint[a]
Gly^6	$H^{\alpha*}$	$-Met^8$	H^N	weak
Gly^6	H^N	$-Asp^9$	$H^{\beta1}$	medium
Gly^6	H^N	$-Asp^9$	$H^{\beta2}$	medium
Met^8	H^α	$-Arg^{10}$	H^N	medium
Ile^{11}	$H^{\delta1*}$	$-Tyr^{14}$	H^N	weak
Cys^{13}	H^N	$-Ile^{11}$	$H^{\gamma2*}$	weak
Cys^{13}	H^α	$-Ile^{11}$	$H^{\delta1*}$	weak
Cys^{13}	$H^{\beta1}$	$-Ile^{11}$	$H^{\delta1*}$	weak
Cys^{13}	$H^{\beta2}$	$-Ile^{11}$	$H^{\delta1*}$	weak
long-range NOE connectivity				
proton		−proton		NOE restraint[a]
Cys^2	$H^{\beta1}$	$-Ile^{11}$	$H^{\gamma2*}$	weak
Cys^2	$H^{\beta2}$	$-Ile^{11}$	$H^{\gamma2*}$	weak
Cys^2	$H^{\beta1}$	$-Ile^{11}$	$H^{\delta1*}$	weak
Cys^2	$H^{\beta2}$	$-Ile^{11}$	$H^{\delta1*}$	weak
His^3	H^N	$-Ile^{11}$	$H^{\gamma2*}$	weak
Phe^4	$H^{\delta*}$	$-Asp^9$	H^α	weak
Phe^4	H^α	$-Ile^{11}$	H^α	medium
Phe^4	H^α	$-Ile^{11}$	$H^{\gamma2*}$	weak
Phe^4	$H^{\beta1}$	$-Ile^{11}$	$H^{\gamma2*}$	weak
Phe^4	$H^{\beta2}$	$-Ile^{11}$	$H^{\gamma2*}$	weak
Phe^4	$H^{\delta*}$	$-Ile^{11}$	H^β	weak
Phe^4	$H^{\delta*}$	$-Ile^{11}$	$H^{\gamma11}$	weak
Phe^4	$H^{\delta*}$	$-Ile^{11}$	$H^{\gamma12}$	weak
Phe^4	$H^{\delta*}$	$-Ile^{11}$	$H^{\gamma2*}$	weak
Phe^4	$H^{\delta*}$	$-Ile^{11}$	$H^{\delta1*}$	weak

[a] Weak and medium represent the classification of the NOE distance restraint as described in the Experimental Section.

Table 3. Backbone RMSD and Inter-C^α and Inter-C^β Distance between Phe4 and Ile11

	rmsd (Å)			distance[b] (Å)	
peptide	1−15[a]	2−13[a]	6−9[a]	Phe^4 C^α−Ile11 C^α	Phe^4 C^β−Ile11 C^β
aqueous solution					
1	2.84	2.25	1.31	12.89(1.74)	14.54(2.42)
3	2.49	1.85	1.25	6.85(0.59)	7.34(0.57)
4	3.50	2.74	1.19	10.87(1.43)	11.57(1.90)
5	3.54	2.84	1.15	7.67(1.76)	7.03(1.09)
DMSO solution					
1	2.22	1.17	0.38	5.11(0.11)	5.75(0.39)
3	1.05	0.58	0.16	4.46(0.18)	4.95(0.36)

[a] Numbers indicate aligned residues. [b] Values in parentheses are standard deviations.

backbone heavy atoms and the inter-C^α and inter-C^β distances between Phe^4 and Ile^{11} are given in Table 3. Figure 3 shows a superposition of the 10 lowest energy conformations with the lowest rmsd aligned using residues 2−13. Only the region between residues 6−9 of miniANP (**1**) took an ordered conformation in the aqueous solution. On the other hand, miniANP (**1**) took a more ordered conformation in the DMSO solution than in the aqueous solution. The presence of the NOE connectivity between Gly^6 and Asp^9 indicated a turnlike conformation at residues 6−9 in both solutions. However, it could not be defined as a typical turn conformation in the aqueous solution because of a lack of strong intramolecular hydrogen bonds, since an amide proton exchange experiment using the miniANP (**1**) solution indicated that all the NH groups were solvent-exposed (data not shown). On the other hand, the arrangement of Phe^4 and Ile^{11} was significantly different for the aqueous and DMSO solutions. In the DMSO solution,

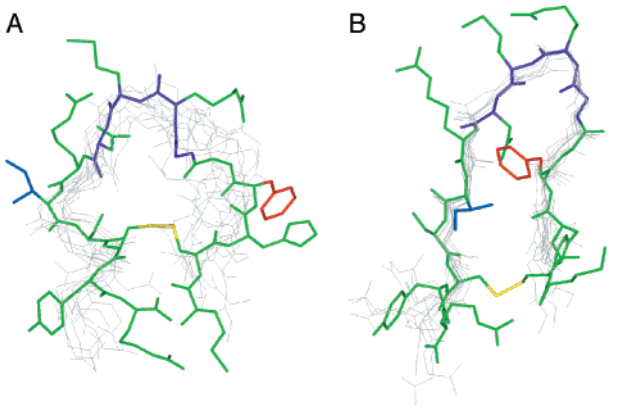

Figure 3. Superposition of the backbone atoms of the 10 lowest energy conformations of miniANP (**1**) in aqueous (A) and DMSO (B) solutions on their mean coordinates, aligned using residues 2−13. The lowest energy conformations with side chains are color-coded. The backbone atoms of residues 6−9 are in magenta, the side chain of Phe^4 is in red, Ile^{11} is in blue, and the disulfide bond is in yellow. Hydrogens are omitted for clarity.

these two residues were located in a proximate position and their hydrophobic side chains were on the same side of the peptide ring, whereas they were not located in such a position in the aqueous solution.

The segment of Phe^4 through Ile^{11} of miniANP (**1**) corresponds to that of Phe^8 through Ile^{15} of ANP (**2**) (Figure 1). However, no NOE connectivity between Phe^8 and Ile^{15} of ANP (**2**) was observed in the DMSO solution,[10] and thus, there was no ring current effect on Ile^{15}. On the other hand, a fairly large difference in the chemical shift of $C^\gamma H_3$ was observed between Ile^{11} of miniANP (**1**) (0.76 ppm) and Ile^{15} of ANP (**2**) (1.08 ppm). When ring current shifts for the 10 lowest energy conformations of miniANP (**1**) in the DMSO solution were calculated with the program MOLMOL,[11] the chemical shift of Ile^{11} $C^\gamma H_3$ was the most affected and showed 0.44 ppm upfield shifts as the average value. This result is consistent with the chemical shift difference of Ile between ANP (**2**) and miniANP (**1**).

The proximate pair of Phe^4 and Ile^{11} was also observed in Phe^8 and Ile^{15} of [Asp^3, Thr^9, Ser^{11}, Leu^{12}, Ser^{14}, Arg^{16}]ANP (ANP hexamutant) in aqueous solution.[12] In light of the importance of the Phe^4, Met^8, and Ile^{11} residues for the activity,[1] the proximate Phe^4−Ile^{11} pair and the turnlike conformation at residues 6−9 are assumed to be correlated with the biological activity.

Restrained Molecular Dynamics Simulation. rMD simulation at 900 K was used to search for favorable ϕ angles of Gly^5 and Gly^6 of miniANP (**1**) under conditions that restrain the turnlike conformation at residues 6−9 and the Phe^4−Ile^{11} pair. Figure 4 shows distributions of the ϕ angles for Gly^5 (A) and Gly^6 (B) of the 100 conformations collected during each rMD simulation. Without the restraints (open bars), the distributions were typical of glycine, at a ratio of 52:48 for Gly^5 and 44:56 for Gly^6 for the positive to negative ϕ angle ratio. With only the restraint for the turn conformation (hatched bars), the minus ϕ angle was dominant for both glycines. With both of the restraints (filled bars), ϕ angles were biased toward positive values, which are typical for D-amino acids, at a ratio of 68:32 for Gly^5 and 78:22 for Gly^6. These results suggested that the ϕ

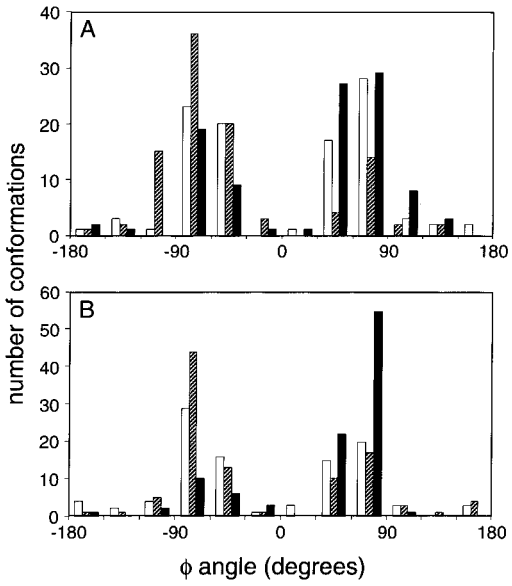

Figure 4. Distribution of the ϕ angles of Gly^5 (A) and Gly^6 (B) in the conformations of miniANP (**1**) generated by rMD simulation. Open bars represent the MD simulation without a restraint, hatched bars represent rMD simulation with restraint I, and filled bars represent rMD simulation with restraints I and II. A total of 100 conformations were sampled for each rMD simulation.

Table 4. Biological Activity of MiniANP (**1**) and the Analogue Peptides

peptide	biological activity, EC_{50} (pmol)	relative biological activity, EC_{50} analogue/EC_{50} miniANP
1	458 ± 11[a]	1
2	120 ± 16	0.27
3	176 ± 39	0.38
4	3760 ± 281	8.2
5	1313 ± 121	2.9

[a] The mean values of two independent experiments.

angles for Gly^5 and/or Gly^6 would prefer positive values when miniANP (**1**) has the turn conformation at residues 6−9 and the Phe^4−Ile^{11} pair.

Designing Analogue Peptides and Biological Activity. Among α-amino acids, glycine is the only one that can take a positive ϕ angle without unfavorable steric interaction. Thus, the necessity for Gly^5 and Gly^6 in miniANP (**1**) may be ascribed to the positive ϕ angle in the receptor-bound conformation. If this is the case, Gly^5 and/or Gly^6 may be substituted with appropriate D-amino acids without loss of biological activity. To test this idea, [D-Ala^5]miniANP (**3**), [D-Ala^6]miniANP (**4**), and [D-Ala^5, D-Ala^6]miniANP (**5**) were synthesized (Figure 1), and their activity in the production of cGMP was examined. [D-Ala^5]miniANP (**3**) had increased biological activity compared to miniANP (**1**), but [D-Ala^6]miniANP (**4**) and [D-Ala^5, D-Ala^6]miniANP (**5**) had decreased activity (Table 4). Thus, the substitution of D-Ala^5 for Gly^5 contributes to the increase in the biological activity, indicating that Gly^5 of miniANP (**1**) prefers a positive ϕ angle upon binding to the receptor, but the methyl group of D-Ala^6 may suppress the binding of the ligand.

Solution Conformations of Analogue Peptides. All the analogue peptides in aqueous solution and [D-Ala^5]miniANP (**3**) in DMSO solution were analyzed by NMR in the same manner. [D-Ala^5]miniANP (**3**) in the aqueous solution showed NOE connectivities between those of Gly^6 and Asp^9 and between those of Phe^4 and Ile^{11}, characteristic for a turnlike conformation at residues 6−9 and a proximate Phe^4−Ile^{11} pair, respectively. In the DMSO solution of [D-Ala^5]miniANP (**3**), an additional NOE connectivity between D-Ala^5 and Asp^9 was observed, and a well-defined structure of the ring region (residues 2−13) was obtained in this case, using the NOE distance restraints summarized in Table 1. On the other hand, [D-Ala^6]miniANP (**4**) in the aqueous solution lacked NOE connectivities between D-Ala^6 and Asp^9 and between Phe^4 and Ile^{11}. [D-Ala^5, D-Ala^6]miniANP (**5**) in the aqueous solution also lacked NOE connectivity between D-Ala^6 and Asp^9 but retained that between Phe^4 and Ile^{11}. Figure 5 shows the superpositions of the 10 lowest energy conformations for four cases. The conformations of [D-Ala^5]miniANP (**3**) in the aqueous and DMSO solutions were similar to that of miniANP (**1**) in the DMSO solution, characterized by a turnlike conformation at residues 6−9 and a proximate Phe^4−Ile^{11} pair (Figure 3B and Figure 5A,B). Restriction of the ϕ angle by the D-Ala substitution for Gly^5 would have a strong influence on the orientation of the side chain of Phe^4. The inter-C$^\alpha$ and inter-C$^\beta$ distances between Phe^4 and Ile^{11} of [D-Ala^5]miniANP (**3**)

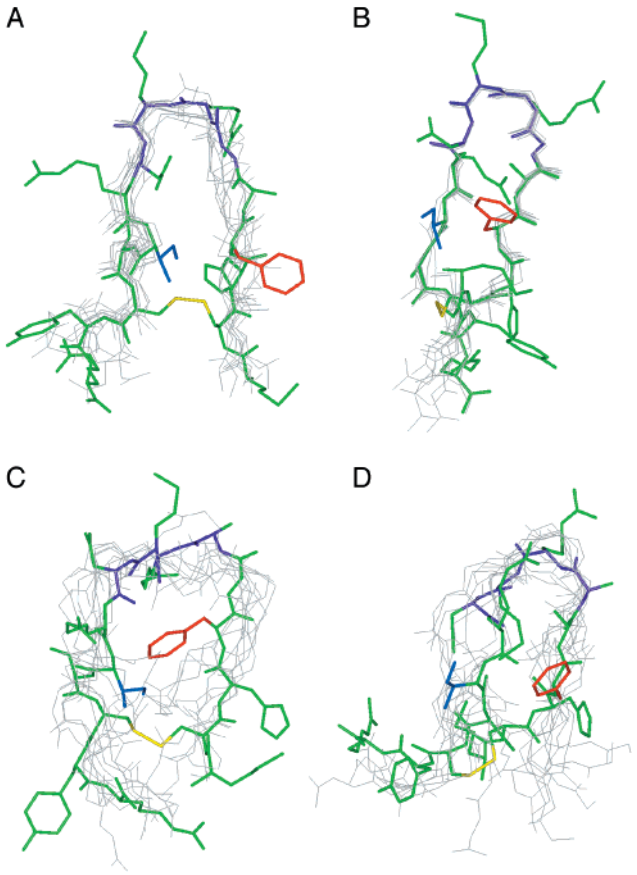

Figure 5. Superposition of the backbone atoms of the 10 lowest energy conformations [D-Ala^5]miniANP (**3**) in aqueous solution (A), [D-Ala^5]miniANP (**3**) in DMSO solution (B), [D-Ala^6]miniANP (**4**) in aqueous solution (C), and [D-Ala^5, D-Ala^6]miniANP (**5**) in aqueous solution (D) on their mean coordinates. Residues 2−13 were used for alignment. The lowest energy conformations with side chains are color-coded. The backbone atoms of residues 6−9 are in magenta, the side chain of Phe^4 is in red, Ile^{11} is in blue, and the disulfide bond is in yellow. Hydrogens are omitted for clarity.

are shorter than those of miniANP (**1**) for both aqueous and DMSO solutions (Table 3). The increased biological activity suggests that D-Ala^5 places the side chains of Phe^4 and Ile^{11} in a proper arrangement for binding to the receptor and that the conformation formed by the Phe^4 and Ile^{11} pair is retained in the receptor-bound conformation. [D-Ala^6]miniANP (**4**) has a distinct conformation in which Phe^4 is distant from Ile^{11} and does not show the turnlike conformation (Figure 5C). [D-Ala^5, D-Ala^6]miniANP (**5**) in aqueous solution showed another conformation in which a turnlike conformation was formed by the main chain at residues 5−8 but not 6−9, although Phe^4 was proximal to Ile^{11} (Figure 5D).

The ϕ angles of Gly^6 in the 10 lowest energy conformations of [D-Ala^5]miniANP (**3**) in the DMSO solution were almost 180°, which are both characteristic of L- and D-amino acid residues (those in aqueous solution did not converge). Even when a model of [D-Ala^5, D-Ala^6]-miniANP (**5**) was constructed from the conformation of [D-Ala^5]miniANP (**3**), the turnlike conformation was not maintained at residues 6−9 and formed at residues 5−8. Therefore, the reduced biological activity of [D-Ala^6]-miniANP (**4**) and [D-Ala^5, D-Ala^6]miniANP (**5**) may be due to interference with D-Ala^6 to form the proper conformation at residues 6−9. On the other hand, D-Ala^5 may contribute to the formation of the proximate Phe^4−Ile^{11} pair. Above all, the D-Ala mutants of miniANP (**1**) support the idea that the turnlike conformation at residues 6−9 and the proximate Phe^4−Ile^{11} pair are important for the receptor-bound conformation of mini-ANP (**1**).

Recently, the crystal structure of the dimerized ligand-binding domain of NPR-A was determined at 2.0 Å resolution.[13] Although affinity labeling studies indicated that ANP (**2**) binds near Met^{173} and His^{195} of NPR-A, the receptor-bound conformation of ANP (**2**) or miniANP (**1**) is still unknown. We carried out a docking simulation of NPR-A and [D-Ala^5]miniANP (**3**) with the program Affinity in the INSIGHT II 98.0 package. The coordinates of NPR-A in the Protein Data Bank (accession number 1DP4) and the lowest energy conformation of [D-Ala^5]miniANP (**3**) in aqueous solution were used for the docking study. [D-Ala^5]miniANP (**3**) formed a complex near Met^{173} and His^{195} of NPR-A in which the three Arg residues in [D-Ala^5]miniANP (**3**) were found at the binding site and the Phe^4−Ile^{11} pair was exposed to the surface. This model suggested that electrostatic interactions are more preferable than van der Waals interactions at the receptor-binding site.

Discussion

Most small peptides would interconvert several conformations rapidly in solution. Judging from the line width of the NOESY spectrum in the DMSO solution (Figure 2B), miniANP (**1**) also would interconvert several conformations. Thus, it should be noted that the conformation presented in this study would be an average conformation. However, the existence of the NOEs indicates undoubted evidence that the parent proton atoms are proximal in similar conformations. The turnlike conformation and the proximate Phe^4−Ile^{11} pair are constructed from NOEs between Gly^6 and Asp^9 and between Phe^4 and Ile^{11}. These conformational properties would be characteristic of the conformation of miniANP, which may correlate with the biological activity.

Conformations of ANP (**2**) have been investigated in several environments such as aqueous solution, DMSO solution, and sodium dodecyl sulfate micelles.[14−17] Although these studies showed that ANP (**2**) has several regions with well-defined structures, they failed to elucidate the overall conformation. Later, a hexamutant that is as potent as wild-type ANP (**2**) in stimulating NPR-A guanylyl cyclase activity was analyzed in aqueous solution and its overall conformation was determined.[12,18] However, the conformation differed significantly from that of the well-defined regions of ANP (**2**) mentioned above. Comparison of [D-Ala^5]miniANP (**3**) with the corresponding region of the ANP hexamutant shows that the proximate pair of the Phe and Ile residues is a common feature (see Figure 6 in ref 10).

Some peptides form amphiphilic conformations or hydrophobic clusters in DMSO.[19,20] As for ANP (**2**), long-range NOE connectivities could be observed only at high viscosity of the sample solution at low temperature (in DMSO solution at 30 mM and at 19.5 °C).[10] Therefore, the higher viscosity of DMSO than of H_2O would induce an amphiphilic conformation to form the proximate Phe^4−Ile^{11} pair of miniANP (**1**).

Structure−activity relationships have been widely used with various ANP analogues to gain insight into biological mechanisms. Bovy et al. synthesized analogue peptides of ANP to identify the structural requirement for ANP receptor subtypes.[9] They concluded that the structural elements responsible for binding to NPR-A span the entire sequence of ANP (**2**), and the sequence Gly^{10} to Gly^{16} plays an important role in the recognition by the receptor. von Geldern et al. synthesized 64 ANP (**2**) analogues of various lengths in order to develop small ANP analogues.[21] Their study on the analogues showed that the orientation of the side chain of Phe^8 (Phe^4 of miniANP (**1**)) was critical for biological activity. This is consistent with the result that the location of Phe^4 and Ile^{11} of miniANP (**1**) is essential for the biological activity. The necessity of the small size or flexibility of Gly^6 of miniANP (**1**) is also consistent with the decrease in activity of the D-Ala^9−Ala^{10} analogue.

It has been reported that ANP (**2**) is inactivated in the renal brush border membrane and in vivo by neutral endopeptidase 24.11 (NEP).[22,23] However, the peptidase-resistant nature of D-amino acids would not contribute to the increase in the biological activity of [D-Ala^5]-miniANP (**3**), since CHO cells do not clear ANP (**2**). Nevertheless, the possibility that other proteases secreted by the CHO cells could degrade the peptides is not completely ruled out.

In the present study, three Gly^5−Gly^6 analogues were designed on the basis of the solution conformations and rMD simulations of miniANP (**1**), and one of the three analogues showed stronger biological activity than the original peptide. Thus, in conjunction with the monovalent phage display, the three-dimensional structure is indispensable for designing analogues efficiently.

Conclusion

In this study, the receptor-bound property of miniANP (**1**) has been investigated by NMR combined with

restrained molecular dynamics (rMD) simulation, amino acid replacements, and examination of biological activity. The obtained structural information was used to design a miniANP analogue with potent biological activity. The solution conformations elucidated by NMR analysis showed two characteristic conformations: a turnlike conformation at residues 6−9 and a proximate pair formed by the side chains of Phe^4 and Ile^{11}. These two conformations were assumed to be receptor-bound properties. An rMD simulation was carried out to search for favorable conformations, especially the flexible sequence of Gly^5−Gly^6. It suggested that the positive ϕ angles for these residues favor the turnlike conformation and the proximate pair. The validity of the preference in the ϕ angles deduced from the rMD was assessed on the basis of the biological activity and solution conformations of model analogue peptides, [D-Ala^5]miniANP (**3**), [D-Ala^6]miniANP (**4**), and [D-Ala^5, D-Ala^6]miniANP (**5**). The solution conformation of [D-Ala^5]miniANP (**3**), which has a higher level of activity than miniANP (**1**), showed the proximate pair in addition to the turnlike conformation. On the other hand, a less active [D-Ala^6]-miniANP (**4**) showed neither the proximate Phe^4−Ile^{11} pair nor the turnlike conformation. Therefore, these two conformations and the positive ϕ angle for Gly^5 were concluded to be necessary for the receptor-bound conformation. The reduced activity of [D-Ala^6]miniANP (**4**) may indicate that the small size of Gly^6 is required for a compact conformation.

Combining such structural information with the crystal structure of the ligand-binding domain, we will be able to elucidate the roles of the amino acid residues in receptor binding. A further optimization of the peptide structure using modified amino acid analogues may lead to the design of new peptide and non-peptide ANP analogues.

Experimental Section

Materials. miniANP (**1**) was synthesized using FastMoc chemistry by a solid-phase peptide synthesizer (model 433A PE Biosystems, Tokyo, Japan). After the formation of a disulfide bond by dimethyl sulfoxide (DMSO)/HCl, miniANP (**1**) was purified by high-performance liquid chromatography (HPLC) with a C-18 reversed-phase column (Capcell pack C18 UG80 20 mm × 250 mm, Shiseido, Tokyo, Japan). Analogue peptides were purchased from Peptide Institute, Inc. (Osaka, Japan). The sample concentration was 2.0 mM unless otherwise stated. The pH value of all aqueous solutions (90% H_2O/10% D_2O) was approximately 3 to observe amide signals.

NMR Measurements and Structure Calculations. NMR experiments were carried out on a Bruker DMX 750 spectrometer at 25 °C. Experimental parameters for DQF-COSY,[24] TOCSY,[25,26] and NOESY[27,28] were as follows. The spin-lock period in TOCSY was 65 ms, and the mixing times in NOESY were 50, 100, 150, 200, 250, and 300 ms. The 2D NMR spectra were recorded using time-proportional phase incrementation (TPPI) for quadrature detection in the F_1 dimension.[29] Data points are 512 and 2048 for the t_1 and t_2 dimensions, respectively. Thirty-two transients were accumulated for each acquisition with a 2.0 s relaxation delay. The spectral width was adjusted between 7508 and 10 504 Hz in order to observe all the proton signals. The data were apodized with a sine-bell window function and zero-filled to a matrix size of 2K × 2K data points before Fourier transformation. Proton signals were assigned using the conventional assignment strategy[30,31] with the FELIX 98.0 software package (MSI, San Diego, CA). Spin system assignments were performed using 2D DQF-COSY and TOCSY spectra. A 2D NOESY spectrum collected with a mixing time of 300 ms was used to identify sequential backbone connectivities. Side chain proton resonances of all residues were unambiguously identified from the 2D TOCSY spectrum. NOE connectivities and their build-up curves were obtained from the 2D NOESY spectra collected with mixing times of 50, 100, 150, 200, 250, and 300 ms. These build-up curves were converted into upper-bound distance restraints classified as strong, medium, or weak, corresponding to 2.7, 3.7, or 5.0 Å, respectively. Pseudoatom corrections were added to upper-bound distance restraints if necessary. The lower bound distance restraints were set to 1.8 Å, representing the sum of van der Waals radii of the interacting atoms. Intraresidue NOE connectivities that would not affect the structure calculation were excluded.

Structure calculations were carried out using simulated annealing[32] with the program NMRchitect in the INSIGHT II 98.0 package (MSI). The energy of the system was calculated with the AMBER force field.[33,34] The NOE force constant was set to 30.0 kcal $Å^{-2}$, and the force constant for the dihedral angle ω was set to 100 kcal rad^{-2} to maintain the trans configuration of the peptide bond. The calculation started with energy minimization under the condition that all the force constants were reduced to 0.001 kcal mol^{-1} $Å^{-2}$. Then, MD with the weak force field was initiated at 1000 K so that the molecule could access a wide conformational space. All the force constants except for nonbond terms (van der Waals interaction) were scaled up to their full values gradually during this MD phase, and the molecule was loosely folded. The structure was refined in a second stage of dynamics with the nonbond terms increasing to their full values during gradual cooling to 298 K. Finally, energy minimization was applied.

All the calculations were performed on a Silicon Graphics OCTANE workstation.

Restrained Molecular Dynamics Simulation. rMD simulations were performed using the program DISCOVER 3 in the INSIGHT II 98.0 package. The energy of the system was calculated with the AMBER force field. A cutoff of 12.0 Å was used for the nonbonded energy evaluation, and a distance-dependent dielectric constant ($\epsilon = 4r$) was used to compensate for the lack of explicit solvent. The force constants of distance and dihedral angle restraints were set to 30 kcal $Å^{-2}$ and 100 kcal rad^{-2}, respectively.

rMD simulations were applied to the NMR structure with the lowest energy. Restraints used were as follows. (I) A hydrogen bond between Gly^6 CO and Asp^9 NH was introduced to form a βI turn conformation at residues 6−9. The distance restraints were set to 2.12 Å for O···H and 3.05 Å for O···N, and the angle restraints were set to 116° for C−O···H and 155° for O···H−N.[35] (II) The side chains of Phe^4 and Ile^{11} were arranged proximal to each other. Inter-C^α and inter-C^β distances between Phe^4 and Ile^{11} were set to 5.11 and 5.75 Å, respectively, which were those of the mean values of the 10 lowest energy conformations of miniANP (**1**) in DMSO solution (Table 3). The simulation started with the assignment of random velocities to atoms followed by equilibration of the system at 900 K for 10 ps. After the equilibration, the coordinates of the structure were collected. This rMD simulation at 900 K was repeated 100 times to search for various conformations. Then each conformation was subjected to a second rMD simulation under the same conditions except for temperature, which was changed from 900 to 298 K. After the reequilibration interval at 298 K, the energy of each conformation was minimized until the maximum derivative decreased to below 0.001 kcal mol^{-1} $Å^{-1}$.

Intracellular Cyclic GMP Measurement. Cloning and expression of the human NPR-A cDNA in Chinese hamster ovary (CHO) cells have been described by Kitano et al.[36] A stable tansfectant expressing human NPR-A (CHO/A) was used to determine the agonist potencies of miniANP (**1**) or analogue peptides. CHO/A cells were cultured in a-MEM lacking ribonucleosides and deoxyribonucleoside (Life Technologies Oriental Inc., Tokyo, Japan) supplemented with 10% dialyzed fetal bovine serum. The 1×10^4 CHO/A cells were preincubated with 0.5 mM 3-isobutyl-L-methylxanthine at 37

°C for 15 min and incubated with various concentrations of peptides at 37 °C for 30 min. The amounts of intracellular cGMP were measured by radioimmunoassay with Yamasa cyclic cGMP assay kits (Yamasa, Chiba, Japan).

Abbreviations. Abbreviations for common amino acids are in accordance with the recommendations of IUPAC. Additional abbreviations are the following: ANP, atrial natriuretic peptide; rMD, restrained molecular dynamics; NPR, natriuretic peptide receptor; cGMP, cyclic guanosine 5′-monophosphate; NOE, nuclear Overhauser effect; DMSO, dimethyl sulfoxide; DQF-COSY, double quantum filtered correlation spectroscopy; TOCSY, total correlation spectroscopy; NOESY, nuclear Overhauser effect spectroscopy; RMSD, root-mean-square deviation.

Acknowledgment. This research was supported by the special coordination fund for the promotion of science and technology from the science and technology agency of Japan. We thank Dr. Hiroyuki Minakata for advice regarding peptides including D-amino acids.

Supporting Information Available: Lists of proton resonance assignments for miniANP (**1**) and analogue peptides, fingerprint regions of 2D NOESY spectra of analogue peptides, $\phi-\psi$ angles at each residue, and disulfide χ angles for the lowest energy conformation of each peptide. This material is available free of charge via the Internet at http://pubs.acs.org.

References

(1) Li, B.; Tom, J. Y.; Oare, D.; Yen, R.; Fairbrother, W. J.; Wells, J. A.; Cunningham, B. C. Minimization of a polypeptide hormone. *Science* **1995**, *270*, 1657−1660.
(2) Kangawa, K.; Matsuo, H. Purification and complete amino acid sequence of alpha-human atrial natriuretic polypeptide (alpha-hANP). *Biochem. Biophys. Res. Commun.* **1984**, *118*, 131−139.
(3) Levin, E. R.; Gardner, D. G.; Samson, W. K. Natriuretic peptides. *N. Engl. J. Med.* **1998**, *339*, 321−328.
(4) Koller, K. J.; Goeddel, D. V. Molecular biology of the natriuretic peptides and their receptors. *Circulation* **1992**, *86*, 1081−1088.
(5) Garbers, D. L. The guanylyl cyclase receptor family. *New Biol.* **1990**, *2*, 499−504.
(6) Iwata, T.; Uchida-Mizuno, K.; Katafuchi, T.; Ito, T.; Hagiwara, H.; Hirose, S. Bifunctional atrial natriuretic peptide receptor (type A) exists as a disulfide-linked tetramer in plasma membranes of bovine adrenal cortex. *J. Biochem.* **1991**, *110*, 35−39.
(7) Lowe, D. G. Human natriuretic peptide receptor-A guanylyl cyclase is self-associated prior to hormone binding. *Biochemistry* **1992**, *31*, 10421−10425.
(8) Chinkers, M.; Wilson, E. M. Ligand-independent oligomerization of natriuretic peptide receptors. Identification of heteromeric receptors and a dominant negative mutant. *J. Biol. Chem.* **1992**, *267*, 18589−18597.
(9) Bovy, P. R.; O'Neal, J. M.; Olins, G. M.; Patton, D. R. Identification of structural requirements for analogues of atrial natriuretic peptide (ANP) to discriminate between ANP receptor subtypes. *J. Med. Chem.* **1989**, *32*, 869−874.
(10) Koyama, S.; Kobayashi, Y.; Ohkubo, T.; Kyogoku, Y.; Sato, A.; Kobayashi, M.; Go, N. The differences in conformation between alpha-human atrial natriuretic polypeptide, alpha-hANP, and its derivative, Met(O)-alpha-hANP, in solution. *Protein Eng.* **1990**, *3*, 393−402.
(11) Koradi, R.; Billeter, M.; Wüthrich, K. MOLMOL: a program for display and analysis of macromolecular structures. *J. Mol. Graphics* **1996** *14*, 51−55.
(12) Fairbrother, W. J.; McDowell, R. S.; Cunningham, B. C. Solution conformation of an atrial natriuretic peptide variant selective for the type A receptor. *Biochemistry* **1994**, *33*, 8897−8904.
(13) van den Akker, F.; Zhang, X.; Miyagi, M.; Huo, X.; Misono, K. S.; Yee, V. C. Structure of the dimerized hormone-binding domain of a guanylyl-cyclase-coupled receptor. *Nature* **2000**, *406*, 101−104.
(14) Theriault, Y.; Boulanger, Y.; Weber, P. L.; Reid, B. R. Two-dimensional 1H-NMR investigation of the water conformation of the atrial natriuretic factor (ANF 101−126). *Biopolymers* **1987**, *26*, 1075−1086.
(15) Gampe, R. T., Jr.; Connolly, P. J.; Rockway, T.; Fesik, S. W. Two-dimensional NMR studies of [Pro-10] atrial natriuretic factor [7−23]. *Biopolymers* **1988**, *27*, 313−321.
(16) Kobayashi, Y.; Ohkubo, T.; Kyogoku, Y.; Koyama, S.; Kobayashi, M.; Go, N. The conformation of alpha-human atrial natriuretic polypeptide in solution. *J. Biochem.* **1988**, *104*, 322−325.
(17) Olejniczak, E. T.; Gampe, R. T., Jr.; Rockway, T. W.; Fesik, S. W. NMR study of the solution conformation of rat atrial natriuretic factor 7−23 in sodium dodecyl sulfate micelles. *Biochemistry* **1988**, *27*, 7124−7131.
(18) Cunningham, B. C.; Lowe, D. G.; Li, B.; Bennett, B. D.; Wells, J. A. Production of an atrial natriuretic peptide variant that is specific for type A receptor. *EMBO J.* **1994**, *13*, 2508−2515.
(19) Akasaka, K.; Inoue, T.; Tamura, A.; Watari, H.; Abe, K.; Kainosho, M. Internal motion of a tryptophan residue in Streptomyces subtilisin inhibitor: deuterium nuclear magnetic resonance in solution. *Proteins* **1988**, *4*, 131−136.
(20) Tancredi, T.; Zanotti, G.; Rossi, F.; Benedetti, E.; Pedone, C.; Temussi, P. A. *Biopolymers* **1989**, *28*, 513−523.
(21) von Geldern, T. W.; Rockway, T. W.; Davidsen, S. K.; Budzik, G. P.; Bush, E. N.; Chu-Moyer, M. Y.; Devine, E. M., Jr.; Holleman, W. H.; Johnson, M. C.; Lucas, S. D.; Pollock, D. M.; Smital, J. M.; Thomas, A. M.; Opgenorth, T. J. Small atrial natriuretic peptide analogues: design, synthesis, and structural requirements for guanylate cyclase activation. *J. Med. Chem.* **1992**, *35*, 808−816.
(22) Olins, G. M.; Spear, K. L.; Siegel, N. R.; Zurcher-Neely, H. A. Inactivation of atrial natriuretic factor by the renal brush border. *Biochim. Biophys. Acta* **1987**, *901*, 97−100.
(23) Erdös, E. G.; Skidgel, R. A. Neutral endopeptidase 24.11 (enkephalinase) and related regulators of peptide hormones. *FASEB J* **1989**, *3*, 145−151.
(24) Rance, M.; Sørensen, O. W.; Bodenhausen, G.; Wagner, G.; Ernst, R. R.; Wüthrich, K. Improved spectral resolution in cosy 1H NMR spectra of proteins via double quantum filtering. *Biochem. Biophys. Res. Commun.* **1983**, *117*, 479−485.
(25) Braunschweiler, L.; Ernst, R. R. Coherence transfer by isotropic mixing: application to proton correlation spectroscopy. *J. Magn. Reson.* **1983**, *53*, 521−528.
(26) Bax, A.; Davis, D. G. MLEV-17-based two-dimensional homonuclear magnetization transfer spectroscopy. *J. Magn. Reson.* **1985**, *65*, 355−360.
(27) Kumar, A.; Ernst, R. R.; Wüthrich, K. A two-dimensional nuclear Overhauser enhancement (2D NOE) experiment for the elucidation of complete proton−proton cross-relaxation networks in biological macromolecules. *Biochem. Biophys. Res. Commun.* **1980**, *95*, 1−6.
(28) Bodenhausen, G.; Kogler, H.; Ernst, R. R. Selection of coherence-transfer pathways in NMR pulse experiments. *J. Magn. Reson.* **1984**, *58*, 370−388.
(29) Marion, D.; Wüthrich, K. Application of phase sensitive two-dimensional correlated spectroscopy (COSY) for measurements of 1H−1H spin−spin coupling constants in proteins. *Biochem. Biophys. Res. Commun.* **1983**, *113*, 967−974.
(30) Billeter, M.; Braun, W.; Wüthrich, K. Sequential resonance assignments in protein 1H nuclear magnetic resonance spectra. Computation of sterically allowed proton−proton distances and statistical analysis of proton−proton distances in single crystal protein conformations. *J. Mol. Biol.* **1982**, *155*, 321−346.
(31) Wüthrich, K. *NMR of Proteins and Nucleic Acids*; John Wiley and Sons: New York, 1986.
(32) Nilges, M.; Clore, G. M.; Gronenborn, A. M. Determination of three-dimensional structures of proteins from interproton distance data by dynamical simulated annealing from a random array of atoms. Circumventing problems associated with folding. *FEBS Lett.* **1988**, *239*, 129−136.
(33) Weiner, S. J.; Kollman, P. A.; Case, D. A.; Singh, U. C.; Ghio, C.; Alagona, G. S.; Profeta, J.; Weiner, P. A new force field for molecular mechanical simulation of nucleic acids and proteins. *J. Am. Chem. Soc.* **1984**, *106*, 765−784.
(34) Weiner, S. J.; Kollman, P. A.; Nguyen, D. T.; Case, D. A. An all atom force field for simulations of proteins and nucleic acids *J. Comput. Chem.* **1986**, *7*, 230−252.
(35) Baker, E. N.; Hubbard, R. E. Hydrogen bonding in globular proteins. *Prog. Biophys. Mol. Biol.* **1984**, *44*, 99−179.
(36) Kitano, K.; Fukuda, Y.; Nagahira, K.; Nasu, T.; Izumi, R.; Kawashima, K.; Nakanishi, T. Production and characterization of monoclonal antibodies against human natriuretic peptide receptor-A or -B. *Immunol. Lett.* **1995**, *47*, 215−222.

JM010106K